An Experimental Study of Emulsion Phase Behavior and Viscosity for Athabasca Bitumen/Diethylamine/Brine Mixtures

Kwang Hoon Baek, Francisco J. Argüelles-Vivas, Ryosuke Okuno, Kai Sheng, Himanshu Sharma,
and **Upali P. Weerasooriya,** University of Texas at Austin

Summary

Water is the most dominant component in steam-based oil-recovery methods, such as steam-assisted gravity drainage (SAGD). The central question that motivated this research is whether in-situ bitumen transport in SAGD can be substantially enhanced by generating oil-in-water emulsion, in which the water-continuous phase acts as an effective bitumen carrier. As part of the initial stage of the research project, the main objective of this paper is to present the ability of organic alkali to form oil-in-water emulsions that are substantially less viscous than the original bitumen. Diethylamine (DEA) was used as the organic alkali in this research.

Experimental studies were conducted for emulsion phase behavior and viscosity for mixtures of Athabasca bitumen, DEA, and sodium chloride (NaCl) brine. Experimental variables included brine salinity, alkali concentration, water/oil ratio (WOR), temperature, and sample-aging time.

The phase-behavior study indicated that conditions conducive to oil-in-water emulsions are low alkali concentrations at salinities less than 1,000 ppm. For example, a single phase of oil-in-water emulsion was observed for 0.5, 1.0, 2.0, and 5.0 wt% DEA with WOR of 7:3 with no NaCl. The emulsion for 0.5 wt% DEA, 1,000 ppm NaCl, and WOR of 7:3 was a single-phase oil-in-water emulsion at temperatures up to 403 K at 35 bar. At lower temperatures, 323 and 298 K, flocculation of emulsions in these samples resulted in the separation between the bitumen-rich and water-rich oil-in-water emulsions. However, essentially all bitumen content was measured from the bitumen-rich oil-in-water emulsion. The oil contents in these emulsions were more than 70 vol% at 298 K and 57 vol% at 323 K.

Viscosities of these oil-in-water emulsions ranged between 85 and 115 cp at 1.0 seconds^{-1} and between 31 and 34 cp at 10.0 seconds^{-1}, at 323 K. At 298 K, they ranged between 105 and 250 cp at 1.0 seconds^{-1} and between 48 and 74 cp at 10.0 seconds^{-1}. Results in this research show that, compared with the original bitumen, bitumen-rich oil-in-water emulsions were less viscous by three to four orders of magnitude at 298 K, and less viscous by two orders of magnitude at 323 K.

Introduction

SAGD is widely used for in-situ recovery of bitumen. In SAGD, steam is injected into the bitumen reservoir through an (upper) horizontal well and forms a steam-saturated zone that is called the steam chamber. At the edge of a steam chamber, the vapor (*V*) phase condenses, and releases its latent heat. The heated oil and steam condensate drain by gravity to the (lower) horizontal well, which is 4 to 8 m below and parallel to the injection well. The main drawbacks of SAGD are the significant use of energy and water resources required to generate steam. There is also a large amount of carbon dioxide emission associated with the steam generation.

A widely used parameter to quantify the energy efficiency of steam-injection processes is the cumulative steam/oil ratio (CSOR), defined as the ratio of the cumulative volume of steam injected (cold water equivalent) to the cumulative volume of bitumen produced. For SAGD to be economically feasible, the energy efficiency measured by CSOR is generally in the range of 3 to 5 m^3/m^3. It is desirable to operate at low chamber temperatures while maintaining economically sustainable rates of oil production so that the CSOR can be reduced. However, SAGD is expected to be even less energy efficient for highly heterogeneous reservoirs to be developed for meeting ever-increasing energy demand (Venkatramani and Okuno 2018). Thus, there is a critical need from both environmental and economic perspectives to reduce CSOR in SAGD.

The volume of produced water is at least a few times greater than the volume of produced oil in SAGD and other steam-based methods (e.g., CSOR of 3 to 5 m^3/m^3). That is, water is by far the most dominant component in these oil-recovery methods (Zhu and Okuno 2016). It is important to consider how we can use the water component and/or the aqueous (*W*) phase to improve the efficiency of steam-based oil-recovery methods. The *W* (condensed-water) phase is not currently used for in-situ bitumen transport. Rather, the presence of the *W* phase adversely affects the oleic-phase (*L*-phase) mobility by reducing the *L*-phase relative permeability (Sharma and Gates 2010; Shi and Okuno 2018).

The central hypothesis in this research is that organic alkalis can enhance in-situ bitumen transport in SAGD. Organic alkalis are expected to have several mechanisms to improve the conventional SAGD when injected with steam. First, organic alkalis create a high-pH solution (pH higher than 11) when mixed with liquid water, which is abundant near the edge of a steam chamber. Then, the *W* phase with high pH value is expected to generate natural surfactants in situ by reacting with acidic components that are commonly present in heavy oil and bitumen. The manner in which in-situ surfactants act varies depending on the phase behavior. However, steam-based recovery methods usually yield low-salinity conditions near thermal fronts, where steam condensate makes for high water saturations. At low-salinity conditions (e.g., less than 1,000 ppm), in-situ surfactants might form an oil-in-water emulsion, which transports bitumen as part of a water-continuous phase instead of a viscous *L* phase. In many studies, it was found that lower salinity is more favorable for creating oil-in-water emulsions than water-in-oil emulsions, with the other conditions being fixed (Cooke et al. 1974; Healy et al. 1976; Bera et al. 2012; Al-Yaari et al. 2015; Fortenberry et al. 2015; Bahmanabadi et al. 2016; Sharma et al. 2018).

Second, once organic alkali is condensed near the edge of a steam chamber, it can also act as a diluent for the bitumen. That is, the excess amount of organic alkali residing in the *L* phase can reduce the bitumen viscosity, in addition to the potential mechanisms associated with in-situ surfactants.

This paper (SPE 189768) was accepted for presentation at the SPE Canada Heavy Oil Technical Conference, Calgary, 13–14 March 2018, and revised for publication. Original manuscript received for review 27 December 2017. Revised manuscript received for review 11 July 2018. Paper peer approved 13 July 2018.

Third, organic alkalis would largely be consumed in the reactions for natural surfactants; that is, there would be little or no need to recycle the injectant, unlike the conventional solvent SAGD using alkane-based solvents.

Many researchers have studied the emulsification of heavy oil using different methods for different purposes, as described here. Alkali injection for heavy-oil recovery has been studied in waterflooding processes, such as alkaline/surfactant, alkaline/surfactant/polymer, and alkaline/cosolvent/polymer flooding (Liu et al. 2006, 2007; Bryan and Kantzas 2007a, b; Bryan et al. 2008; Dong et al. 2009; Kumar et al. 2012; Pei et al. 2013; Fortenberry et al. 2015; Zhang et al. 2016; Xiao et al. 2017; Sharma et al. 2018). In these prior studies, different combinations of alkalis, salts, surfactants, cosolvents, and polymers were tested to achieve in-situ conditions for ultra-low interfacial tension (IFT). For pipeline transportation of heavy oil, oil-in-water-emulsion viscosity was studied with different surfactants, alkalis, and solvents at different WORs and shear rates (Ghannam and Esmail 2007; Ashrafizadeh and Kamran 2010; Hasan et al. 2010; Abdurahman et al. 2012; Ashrafizadeh et al. 2012; Ghannam et al. 2012).

Surfactants have been also studied as steam additives for SAGD and cyclic steam stimulation (Srivastava and Castro 2011; Gupta and Zeidani 2013; Lu et al. 2017). These researchers used commercially available hydrophilic viscosity reducers (Lu et al. 2017), hydrophilic surfactants (Gupta and Zeidani 2013), and thin-film-spreading agents (Srivastava and Castro 2011) to form oil-in-water emulsions or to demulsify water-in-oil emulsions to enhance bitumen transport. The potential mechanisms for lowering CSOR by injecting these surfactants with steam include the wettability alteration from oil-wetting to more water-wetting, and reduction of IFT.

Inorganic alkali has been studied for oil-in-water emulsification by natural surfactants (Acevedo et al. 2001; Ashrafizadeh et al. 2012). With no additional surfactants or solvents, these studies used sodium carbonate to activate natural surfactants and create oil-in-water emulsions from Iranian heavy crude oil (Ashrafizadeh et al. 2012) and Cerro Negro bitumen (Acevedo et al. 2001). In both studies, oil-in-water emulsions were observed at the sodium carbonate concentration range from 2,000 to 10,000 ppm.

To our knowledge, Kim et al. (2017) is the only research published on alkali/steam coinjection for SAGD. They injected steam with an alkali (not specified) into a micromodel chip, and observed significantly increased oil recovery by creating oil-in-water emulsions. Although the size of emulsion droplets was studied, Kim et al. (2017) did not study the phase behavior and rheology of emulsions created in their experiment.

Bitumen is a complex mixture of hydrocarbons containing asphaltenes and resins at high concentrations. These components are known to interact with water and to affect emulsion behavior (Schorling et al. 1999; Yan et al. 1999; Yarranton et al. 2000; Xia et al. 2004; Kokal 2005; Yang et al. 2007; Al-Sahhaf et al. 2008; Kar et al. 2014; Gao et al. 2017; Jia and Okuno 2018). It is important to conduct fundamental experimental research of emulsion phase behavior and viscosity for mixtures of Athabasca bitumen, brine, and organic alkali because such experimental research has not been presented in the literature.

As part of the initial portion of the research motivated by the hypothesis stated previously, the main questions to be addressed in this paper are whether oil-in-water emulsions can be formed by adding the organic alkali DEA to Athabasca bitumen and NaCl brine, and, if so, how much oil is contained in such emulsions, and how mobile are the resulting emulsions. Data for emulsion phase behavior are obtained at different alkali concentrations, WORs, NaCl brine salinities, and temperatures for Athabasca bitumen. Such data will be instrumental to further investigation into optimal application conditions of organic alkalis as steam additives for SAGD.

Materials and Methods

Materials. A sample of dehydrated Athabasca bitumen was used for the experiments in this research. It has a molecular weight of 532 g/mol and a density of 0.985 g/cm^3 at 335 K and atmospheric pressure, as measured by Exova (Edmonton, Alberta, Canada). The saturates/aromatics/resins/asphaltenes analysis showed the following composition: 24.5 wt% saturates, 36.6 wt% aromatics, 21.1 wt% resins, and 17.8 wt% asphaltenes (pentane insoluble). For more information about this bitumen, Baek et al. (2018) presented viscosities and densities of this bitumen sample at temperatures from 316 to 451 K and pressures from 1.6 to 100 bar.

The total acid number was measured to be 3.56 mg potassium hydroxide (KOH)/g oil for this bitumen sample using the method of Fan and Buckley (2007). Cooke et al. (1974) showed that the required acid number for an alkali-based oil-recovery method was 1.5 mg KOH/g oil. Ge et al. (2012) showed in their sandpack-flooding experiment that a higher acid number resulted in a higher oil recovery among four oil samples with acid numbers between 1.85 and 4.66 mg KOH/g oil. Therefore, the acid number of the bitumen sample in this research, 3.56 mg KOH/g oil, indicates that the bitumen contained a sufficient amount of acidic components to create natural surfactants by reacting with organic alkali.

DEA was selected as an organic alkali for this research. It has the chemical formula of $(CH_3CH_2)_2NH$ and molecular weight of 73 g/mol. The DEA sample supplied by Sigma-Aldrich has a purity higher than 99.5%. DEA is one of the suitable organic alkalis that meet the main requirements for organic-alkali/steam coinjection, and is between pentane (n-C_5) and hexane (n-C_6) in terms of volatility. Therefore, it is expected to effectively propagate in the reservoir as part of the vapor phase and to condense at thermal fronts. Also, DEA can create a high-pH aqueous phase when it partitions into the aqueous phase. Sheng (2015) studied whether a high-pH condition in aqueous solution is favorable for creating natural surfactants by reactions of alkali with acidic components in bitumen.

For aqueous solutions, different concentrations of brine were prepared with deionized (DI) water and NaCl. DEA was confirmed to make a high-pH aqueous solution. **Table 1** summarizes that the pH values measured were between 10.4 and 11.5 for 1,000 ppm NaCl brine with 10 different DEA concentrations of 0.5, 1.0, 2.0, 5.0, 10, 20, 30, 50, 70, and 90 wt%. NaCl was the only salt used in this research because the salinity of produced water in SAGD (Alberta, Canada) mainly consists of NaCl and is often less than 1,000 ppm (Petersen and Grade 2011; Razi et al. 2016).

Alkali concentration (wt%)	0.5	1.0	2.0	5.0	10
pH of aqueous phase	10.5	11.2	11.3	11.2	11.5
Alkali concentration (wt%)	20	30	50	70	90
pH of aqueous phase	11.5	11.5	11.5	11.2	10.4

Table 1—pH values at different DEA concentrations in 1,000 ppm NaCl brine, which were measured with no bitumen at 298 K and atmospheric pressure.

Preparation of Emulsion Samples. Emulsion phase behavior was studied at different alkali concentrations, salinities, WORs, temperatures, and aging times at atmospheric pressure. Because of the many experimental variables, phase-behavior tests were conducted in two stages: general-phase-behavior scans followed by more-detailed analyses of specific samples.

The general-scan stage aimed to observe phase behavior at a broad range of conditions and to identify desired conditions in terms of transport of oil in the form of oil-in-water emulsion. Samples were made at 10 different alkali concentrations (0.5, 1.0, 2.0, 5.0, 10, 20, 30, 50, 70, and 90 wt% in the aqueous phase) with four different salinities (0, 1,000, 30,000, and 100,000 ppm) for three different WORs (5:5, 7:3, and 9:1). Conditions for some samples exceeded solubility limits for NaCl, such as samples with 30,000 ppm for 90 wt% DEA and 100,000 ppm for 70 and 90 wt% DEA. Also, seven samples were lost because of mechanical failure of glass pipettes, partly caused by high volatility of DEA at 373 K. In total, 104 different samples were observed at 373 K. By measuring the basicity of samples, all acidic components were confirmed to be consumed in the reaction with the DEA added for all samples in this research.

Each sample was prepared for 4 cm^3 in an acrylic pipette of 10 cm^3. The procedure for preparation of each sample is as follows. First, the tip of a pipette was sealed by flame. Then, a specified mixture of brine, DEA, and bitumen was injected into the pipette. The bitumen was heated up to 353 K before the injection to make it more mobile. After injecting all components, argon gas was injected into the pipette as a blanket gas. Finally, the neck of the pipette was sealed by flame. The samples prepared were aged in an oven at 373 K for a certain time period (e.g., 3 weeks for this general scanning). During the aging period, samples were mixed four times a day. Then, samples were allowed to rest for 2 days before reporting emulsion phase behavior at 373 K.

After the general-phase-behavior scans (as will be explained in the subsection Emulsion Phase Behavior), samples with five alkali concentrations (0.5, 2.0, 5.0, 50, and 90 wt% in the aqueous phase) at 1,000 ppm at WOR of 7:3 were chosen for more-specific analysis. The specific salinity, 1,000 ppm, was chosen because salinities of produced water in SAGD are generally less than 1,000 ppm. The selected WOR, 7:3, corresponds to a typical steam/oil ratio of successful SAGD operations, representing the relative amounts of oil and water in gravity drainage on average. For these specific samples, each sample of 8 cm^3 was prepared in a 10-cm^3 pipette using the same procedure of sample preparation as in the general-scanning stage. These specific samples were observed at three different temperatures (298, 323, and 373 K) and three different aging times (1, 2, and 3 weeks).

Analysis of Emulsion Types and Bitumen Content. Two types of emulsions, water-external and oil-external emulsions, were identified by visual observation and the method of Kumar et al. (2012). In this method, a small amount of emulsion is dropped separately into DI water and toluene. A droplet of oil-in-water emulsion, in which water is the external phase, spreads in DI water but not in toluene. A droplet of water-in-oil emulsion, in which oil is the external phase, behaves in the opposite way.

The oil content in oil-in-water emulsion was measured by demulsifying the emulsion with acidization. For 1 cm^3 of oil-in-water emulsion, 2 cm^3 of 3.5-M hydrochloric acid (HCl) solution was added to make a total solution of 3 cm^3. This mixture of emulsion and HCl was stirred until a transparent water was separated from the bitumen. The volume of bitumen was then obtained by measuring the volume of separated water.

Measurement of Emulsion Viscosity. Emulsion viscosities were measured for the selected samples with a salinity of 1,000 ppm and WOR of 7:3 at five different alkali concentrations (0.5, 2.0, 5.0, 50, and 90 wt% in aqueous phase). An emulsion was sampled from the pipette prepared for a specific sample. Then, viscosities of each sample were measured at 298 and 323 K. Measurements at higher temperatures were avoided because of the excessive vaporization of DEA.

The ARES LS-1 rheometer from TA Instruments was used with 50-mm-diameter parallel bottom and upper plates. Different gap sizes were selected depending on the emulsion viscosity of interest. The gap size was set to 0.4 mm for oil-in-water emulsions and 0.8 mm for water-in-oil emulsions. The range of shear rates in this research was from 0.1 to 100 $seconds^{-1}$. The low limit of torque during the viscosity measurement was set as 0.74 μN·m because viscosities measured with lower torques were not reliable.

Special care was taken to avoid shear-thinning behavior caused by using smaller sample volumes (Tagavifar et al. 2017). In addition, a new sample was used for each measurement to avoid errors caused by the alteration of emulsion rheology through experiencing high shear rates. Viscosities were measured immediately after loading the sample. For viscosity measurement at 323 K, however, samples were placed in the rheometer for several minutes until the rheometer reached the target temperature.

Results and Discussion

Emulsion Phase Behavior. Figs. 1 through 3 present a summary of phase behavior and phase volumes derived from the 104 samples (see subsection Preparation of Emulsion Samples) at 373 K after aging for 3 weeks. For Figs. 1 through 3, phase types were identified depending on the method described previously. In general, observed phase-behavior types can be categorized into seven types, with three types for a single phase and four types for two phases. The single-phase types observed are oil-in-water emulsion, water-in-oil emulsion, and bitumen diluted by DEA. The two-phase types observed are oil-in-water emulsion with an excess oil phase, two oil-in-water emulsions (bitumen-rich and water-rich), water-in-oil emulsion with an excess water phase, and water-in-oil emulsion with oil-in-water emulsion. Note that emulsions in Figs. 1 through 3 are stable kinetically for at least 6 months, but not thermodynamically; hence, two coexisting oil-in-water emulsions were formed through separation of the bitumen-rich and water-rich oil-in-water emulsions, resulting from flocculation of droplets in the water-continuous phase (Bibette et al. 1992; Robins and Hibberd 1998; Ballard et al. 2015).

General observations derived from Figs. 1 through 3 are as follows. First, oil-in-water emulsions were dominant at low alkali concentrations, and water-in-oil emulsion appeared with increasing alkali concentration. At alkali concentrations greater than 90 wt% in the aqueous solution, the single phase observed was highly mobile, similar to a solvent-diluted bitumen phase. Second, the dominant emulsion type was oil-in-water emulsion at low salinities and water-in-oil emulsion at high salinities. Third, with the WOR of 9:1 (Fig. 3), oil-in-water emulsion was lean in bitumen because of a small amount of natural surfactants. The higher salinities of 30,000 and 100,000 ppm make the effective WOR lower by forming a clearer aqueous phase. As a result, the water-in-oil emulsion dominates over the oil-in-water emulsion.

Effects of salinity, WOR, and alkali concentration on the emulsion type presented in the literature are useful to understand the observations made in this research. Many studies have shown the inversion of oil-in-water emulsion to water-in-oil emulsion with increasing salinity (Cooke et al. 1974; Healy et al. 1976; Bera et al. 2012; Al-Yaari et al. 2015; Fortenberry et al. 2015; Bahmanabadi et al. 2016; Sharma et al. 2018). With increasing salinity, the interaction between water molecules and salt ions increases relative to that between water molecules and surfactants. As a result, the IFT between emulsion and oil decreases, whereas the IFT between emulsion and water increases with increasing salinity, as experimentally shown by Healy et al. (1976) and Bera et al. (2012).

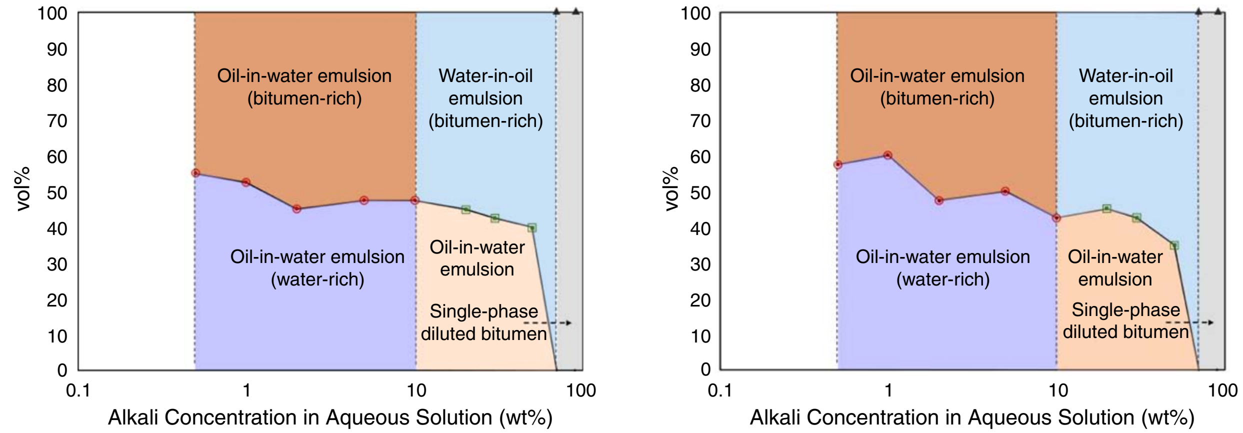

(a) Salinity 0 ppm

(b) Salinity 1,000 ppm

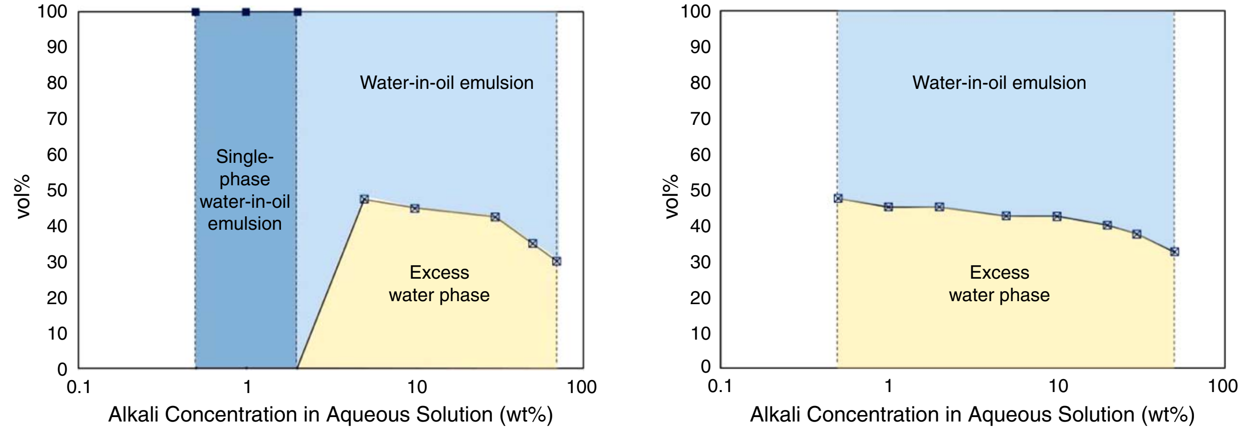

(c) Salinity 30,000 ppm

(d) Salinity 100,000 ppm

Fig. 1—Emulsion phase behavior at the WOR of 5:5 after aging at 373 K for 3 weeks. At salinities of (a) 0 ppm and (b) 1,000 ppm, two oil-in-water emulsions (bitumen-rich and water-rich) were observed up to 10 wt%. Water-in-oil and oil-in-water emulsions were observed from 20 wt%. Note that this water-in-oil emulsion contained nearly all bitumen. For (c) 30,000-ppm samples, a single-phase water-in-oil emulsion was observed at low DEA concentration up to 2.0 wt%. Otherwise, water-in-oil emulsions with an excess water-rich phase were observed. For (d) 100,000-ppm samples, water-in-oil emulsions with an excess water-rich phase were observed. ■ = single-phase water-in-oil emulsion; ▲ = single-phase diluted bitumen; ⦿ = oil-in-water emulsions (bitumen-rich) with oil-in-water emulsions (water-rich); ▣ = water-in-oil emulsions (bitumen-rich) with oil-in-water emulsions (water-rich); ☒ = water-in-oil emulsions with excess water phase.

The inversion of oil-in-water emulsion to water-in-oil emulsion with increasing WOR has been presented by Fortenberry et al. (2015), Bahmanabadi et al. (2016), and Sharma et al. (2018). However, the effect of WOR depends on the oil's properties and therefore the natural surfactants formed by the alkali. By adding different cosolvents, Fortenberry et al. (2015) altered the effect of WOR, where oil-in-water emulsions became more dominant with increasing WOR.

Winsor (1948) showed that the addition of water-soluble organic liquid can invert oil-in-water emulsion to water-in-oil emulsion. In this research, the excess amount of DEA could act as a cosolvent as the alkali concentration increases. Indeed, the inversion from oil-in-water emulsion to water-in-oil emulsion was observed with increasing DEA concentration. This kind of emulsion inversion was also found by Salager et al. (1982), in which oil-in-water emulsions were inverted to water-in-oil emulsions with increasing pentanol concentration at a fixed salinity and WOR.

Table 2 is provided to clearly present the transition of emulsion type (bitumen-rich phase). It shows that oil-in-water emulsion is dominant at low salinity (0 and 1,000 ppm) and low alkali concentration (lower than 10 wt%).

The overall effect of alkali concentration, NaCl concentration, and WOR on emulsion phase behavior showed an optimal range of conditions in terms of the dominance of oil-in-water emulsion for low alkali concentrations for salinities less than 1,000 ppm. Especially at WOR of 7:3, a single phase of oil-in-water emulsion was observed for 0.5, 1.0, 2.0, and 5.0 wt% alkali at 0 ppm and 0.5 wt% alkali at 1,000 ppm **(Figs. 4 and 5).**

The emulsion at 0.5 wt% DEA with 1,000 ppm NaCl and WOR of 7:3 was selected for further analysis at 373, 403, and 443 K at 35 bar, which are relevant to the conditions near the edge of an SAGD chamber. The prepared emulsion sample was stored in an accumulator (instead of a pipette) for experiments at these temperature/pressure conditions. The sample was then transferred to an in-line densitometer (Anton Paar), and densities and saturations were measured for phases in the sample as presented in Sheng et al. (2018). As shown in **Fig. 6,** single-phase oil-in-water emulsions were observed at 373 and 403 K. At 443 K, an oil-in-water emulsion was detected with the excess oil phase. The volumetric concentration of the oil-in-water emulsion was 75 vol%. These results show that oil-in-water emulsions can be created at temperature/pressure conditions relevant to SAGD.

Figs. 7 and 8 show phase behavior of the samples at 1,000 ppm NaCl and WOR of 7:3 at 298 and 323 K. Figs. 7 and 8 can be compared with Figs. 2b and 5 (at 373 K). The comparison indicates that the higher temperature was more favorable for creating single-phase oil-in-water emulsion. For example, the oil-in-water emulsion with 0.5 wt% DEA at 1,000 ppm and WOR of 7:3 showed two phases at 298 and 323 K. However, it became a single-phase oil-in-water emulsion at 373 K. At 35 bar, this oil-in-water emulsion was still a single phase at 403 K (Fig. 6).

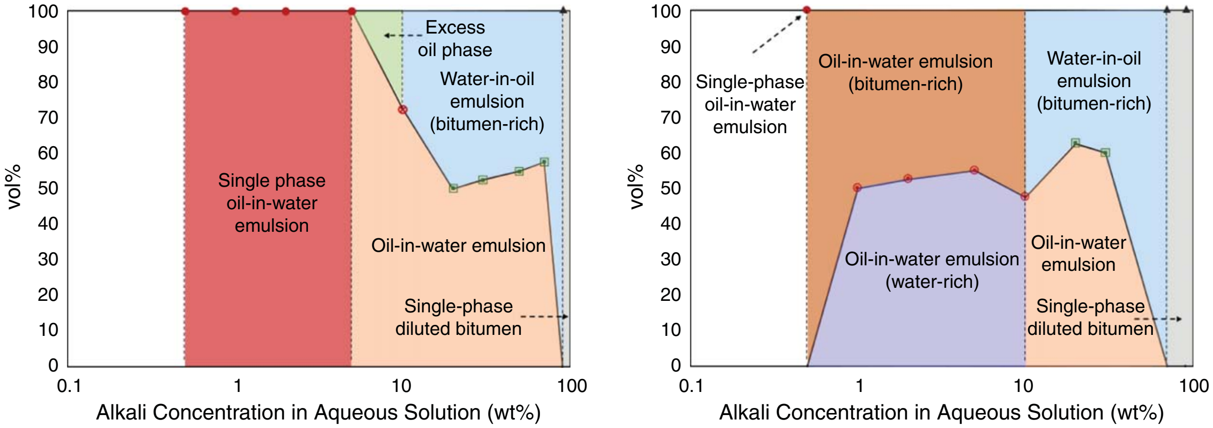

(a) Salinity 0 ppm

(b) Salinity 1,000 ppm

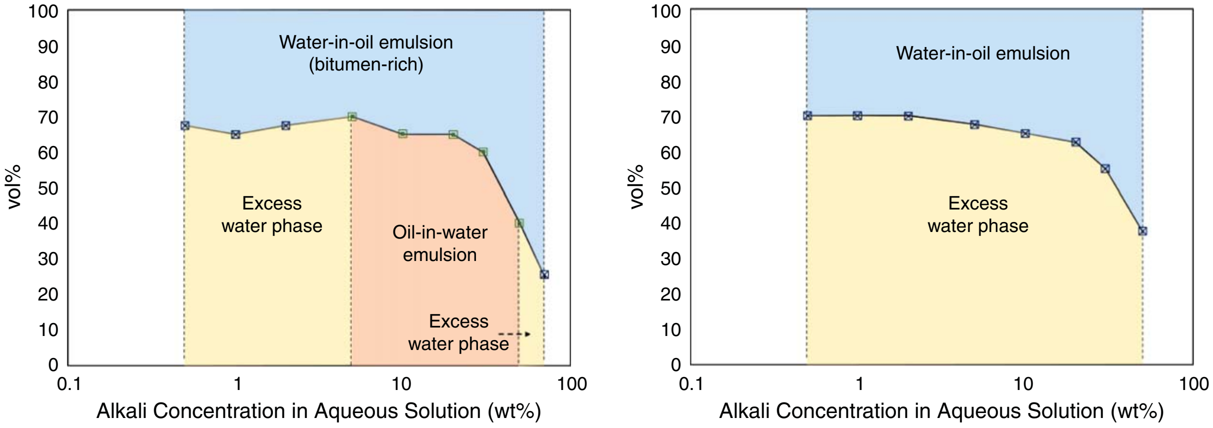

(c) Salinity 30,000 ppm

(d) Salinity 100,000 ppm

Fig. 2—Emulsion phase behavior at the WOR of 7:3 after aging at 373 K for 3 weeks. Single-phase oil-in-water emulsions were observed at low DEA concentrations at salinities of (a) 0 ppm and (b) 1,000 ppm. At 0 ppm, an oil-in-water emulsion phase with an excess oil phase was observed at 10 wt%. At 1,000 ppm, two oil-in-water (bitumen-rich and water-rich) emulsions were observed up to 10 wt% DEA. Two-phase water-in-oil and oil-in-water emulsions were observed from 20 to 70 wt% at both 0 and 1,000 ppm. Note that this water-in-oil emulsion contained nearly all bitumen. For (c) 30,000-ppm samples, water-in-oil emulsion with oil-in-water emulsion or excess water-rich phase was observed. For (d) 100,000-ppm samples, water-in-oil emulsions with excess water-rich phase were observed. ● = a single-phase oil-in-water emulsion; ▲ = a single-phase diluted bitumen; ⊗ = oil-in-water emulsions with excess oil phase; ⦿ = oil-in-water emulsions (bitumen-rich) with oil-in-water emulsions (water-rich); ▣ = water-in-oil emulsions (bitumen-rich) with oil-in-water emulsions (water-rich); ⊠ = water-in-oil emulsions with excess water phase.

Bitumen Content and Viscosity of Oil-in-Water Emulsions. This subsection presents the measurements of bitumen content and the viscosity of oil-in-water emulsions for samples at 1,000 ppm and WOR of 7:3. Phase behavior for these samples was presented in Figs. 2 (373 K) and 7 (298 and 323 K).

The bitumen content was measured for selected samples with alkali concentrations of 0.5, 2.0, and 5.0 wt% at 298 and 323 K after 3 weeks of aging at 373 K. As shown in Fig. 7, there were two emulsions at these conditions: bitumen-rich and water-rich oil-in-water emulsions. Measurement of oil content in each emulsion showed that the bitumen content in the water-rich emulsion was too small to quantify ($<<0.05$ cm^3), and this phase was dark, but still transparent (Fig. 8). Essentially all bitumen content (2.4 cm^3) in the total 8-cm^3 sample was measured from the bitumen-rich oil-in-water emulsion, the volume of which was 3.3 to 3.4 cm^3 at 0.5 to 5.0 wt% DEA at 298 K, and 3.6 to 4.2 cm^3 at 0.5 to 5.0 wt% DEA at 323 K (shown in vol% in Fig. 7). That is, the oil contents in these water-external emulsions were more than 70 vol% at 298 K and 57 vol% at 323 K. The oil content in the emulsion was measured also for samples with shorter periods of aging, of 1 and 2 weeks. However, the effect of aging time on the bitumen content in the emulsion was not observed. From these results, the identification of types "bitumen-rich" and "water-rich" for oil-in-water emulsions was made for Figs. 1, 2, and 7.

Furthermore, emulsion viscosities were measured for samples with alkali concentrations of 0.5, 2.0, 5.0, 50, and 90 wt% at 298 and 323 K after 3 weeks of aging at 373 K. Specifically, measurements were conducted for the bitumen-rich oil-in-water emulsion at 0.5, 2.0, and 5.0 wt% DEA, water-in-oil emulsion at 50 wt% DEA, and the single-phase mixture at 90 wt% (see Fig. 7). Results are presented in **Table 3** and **Fig. 9.** Viscosities of oil-in-water emulsion at different DEA concentrations (0.5, 2.0, and 5.0 wt%) show similar values at a given temperature. This trend could be caused by the similar bitumen content and volumetric concentration for all oil-in-water emulsions. The temperature effect on the viscosity of oil-in-water emulsions is more evident at a higher shear rate (e.g., oil-in-water emulsions at 323 K were less viscous than those at 298 K). Shear-thinning behavior was observed for all fluids studied, indicating hydrodynamic interaction and deformation of dispersed droplets (Pal 1996; Nizamidin et al. 2015). However, the water-in-oil emulsion at the DEA concentration of 50 wt% was only weakly shear-thinning, likely because there was only a small amount of dispersed water in this oil-external emulsion (Pal 2000).

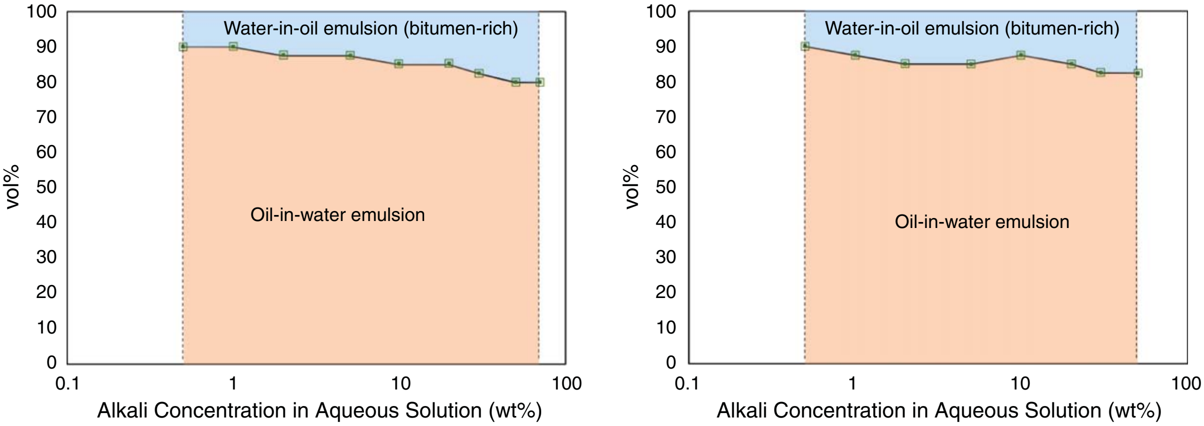

(a) Salinity 0 ppm

(b) Salinity 1,000 ppm

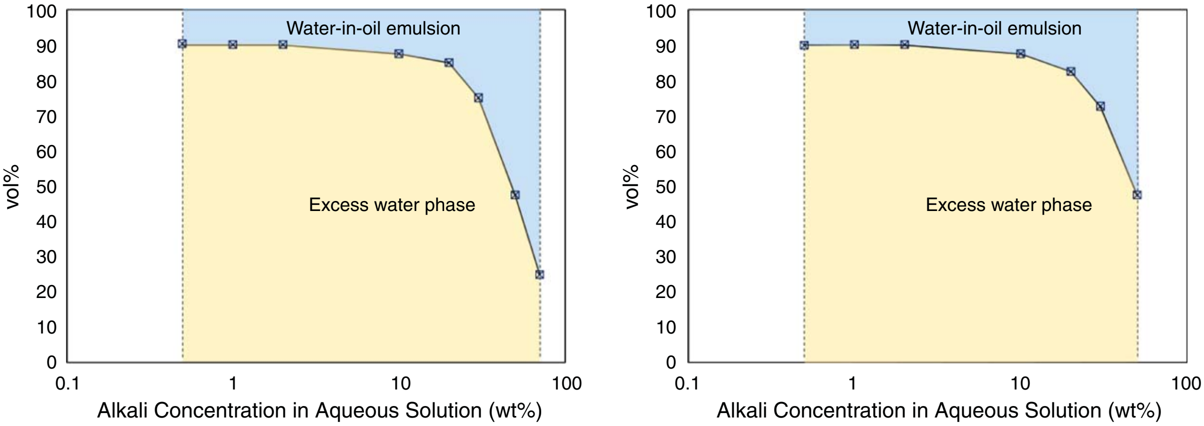

(c) Salinity 30,000 ppm

(d) Salinity 100,000 ppm

Fig. 3—Emulsion phase behavior at the WOR of 9:1 after aging at 373 K for 3 weeks. Two-phase water-in-oil and oil-in-water emulsions were observed for (a) 0-ppm and (b) 1,000-ppm samples. This water-in-oil emulsion contains nearly all bitumen. For (c) 30,000-ppm and (d) 100,000-ppm samples, water-in-oil emulsions with excess water-rich phase were observed. ▣ = water-in-oil emulsions (bitumen-rich) with oil-in-water emulsions (water-rich); ⊠ = water-in-oil emulsions with excess water phase.

The main focus of observation was on the measured viscosities at shear rates less than 10.0 seconds^{-1}, corresponding to in-situ rheological conditions. **Fig. 10** shows the viscosities measured at three shear rates: 1.0, 5.6, and 10.0 seconds^{-1}. Note again that there are three types of fluids in Fig. 10e: bitumen-rich oil-in-water emulsions at DEA concentrations of 0.5, 2.0, and 5.0 wt%; water-in-oil emulsions at 50 wt%; and single-phase mixture at 90 wt%. The single-phase mixture at 90 wt% DEA showed the lowest viscosity at a given shear rate. As expected, the oil-in-water emulsions at low DEA concentrations were less viscous than the water-in-oil emulsions at 50 wt% DEA, reconfirming the identified emulsion types. The viscosities of these oil-in-water emulsions range between 85 and 115 cp at 1.0 seconds^{-1}, and between 31 and 34 cp at 10.0 seconds^{-1} at 323 K. At 298 K, they range between 105 and 250 cp at 1.0 seconds^{-1} and between 48 and 74 cp at 10.0 seconds^{-1}.

The viscosity of the original bitumen was measured to be 9,040 cp at 323 K using the same rheometer (subsection Measurement of Emulsion Viscosity). Newtonian behavior was confirmed for the bitumen sample, as shown in **Fig. 11.** At 298 K, the bitumen viscosity was not measured by the rheometer because of the limitation in torque. However, Baek et al. (2018) presented a viscosity correlation for this bitumen sample using measurements from an in-line viscometer; this correlation provides a viscosity of 447,000 cp at 298 K. Results in this research show that compared with the original bitumen, bitumen-rich oil-in-water emulsions are less viscous by three to four orders of magnitude at 298 K, and less viscous by two orders of magnitude at 323 K.

The water-in-oil emulsion at 50 wt% DEA was more viscous than the oil-in-water emulsions at the lower DEA concentrations. However, the measured viscosities of these water-in-oil emulsions were substantially lower than those of the original bitumen. They range from 135 cp at the shear rate of 10.0 seconds^{-1} to 199 cp at 1.0 seconds^{-1} at 323 K. At 298 K, they range from 1,532 cp at 10.0 seconds^{-1} to 2,218 cp at 1.0 seconds^{-1}. At 50 wt% DEA concentration, an excess amount of DEA diluted bitumen, which lowered the viscosity of the water-in-oil emulsion.

Salinity	0 ppm									
	DEA Concentration (wt%)									
WOR	0.5	1.0	2.0	5.0	10	20	30	50	70	90
5:5	o/w	o/w	o/w	o/w	o/w	w/o	w/o	w/o	dilution	dilution
7:3	o/w	o/w	o/w	o/w	o/w	w/o	w/o	w/o	w/o	dilution
9:1	w/o	w/o	w/o	w/o	w/o	w/o	w/o	w/o	w/o	–

Salinity	1,000 ppm									
	DEA Concentration (wt%)									
WOR	0.5	1.0	2.0	5.0	10	20	30	50	70	90
5:5	o/w	o/w	o/w	o/w	o/w	w/o	w/o	w/o	dilution	dilution
7:3	o/w	o/w	o/w	o/w	o/w	w/o	w/o	–	dilution	dilution
9:1	w/o	w/o	w/o	w/o	w/o	w/o	w/o	w/o	–	–

Salinity	30,000 ppm								
	DEA Concentration (wt%)								
WOR	0.5	1.0	2.0	5.0	10	20	30	50	70
5:5	w/o	w/o	w/o	w/o	w/o	–	w/o	w/o	w/o
7:3	w/o	w/o	w/o	w/o	w/o	w/o	w/o	w/o	w/o
9:1	w/o	w/o	w/o	–	w/o	w/o	w/o	w/o	w/o

Salinity	100,000 ppm							
	DEA Concentration (wt%)							
WOR	0.5	1.0	2.0	5.0	10	20	30	50
5:5	w/o	w/o	w/o	w/o	w/o	w/o	w/o	w/o
7:3	w/o	w/o	w/o	w/o	w/o	w/o	w/o	w/o
9:1	w/o	w/o	w/o	–	w/o	w/o	w/o	w/o

Table 2—Bitumen-rich emulsion types with respect to alkali concentration, WOR, and salinity, from 104 samples. This table clearly shows that oil-in-water emulsion is dominant at low salinity (0 and 1,000 ppm) and low alkali concentration (lower than 10 wt%). The symbol – indicates that the sample was not studied because of mechanical failures of the glass pipettes. o/w = oil-in-water emulsion; w/o = water-in-oil emulsion; dilution = diluted bitumen (not emulsion).

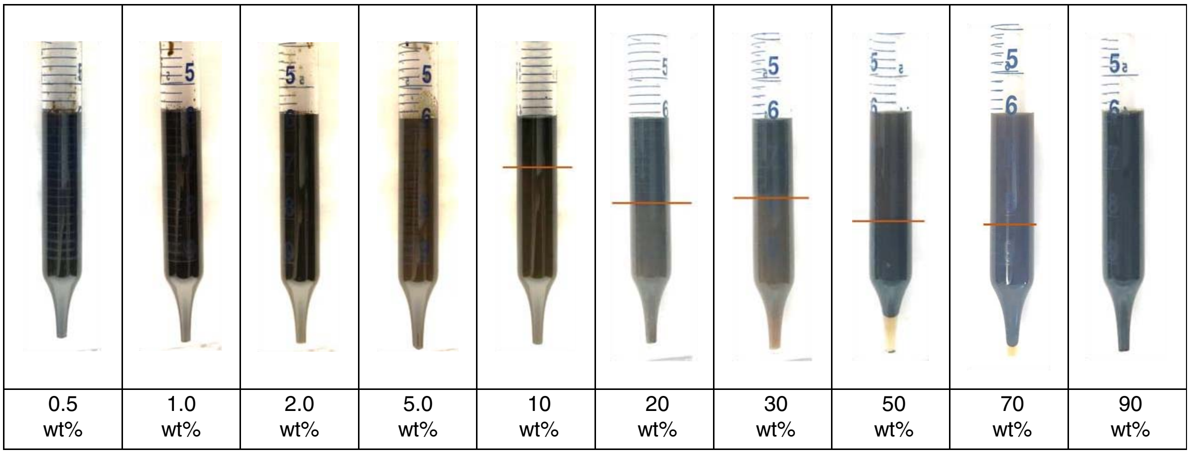

Fig. 4—Emulsion phase behavior at different DEA concentrations with zero salinity and WOR of 7:3, after aging at 373 K for 3 weeks. From 0.5 to 5.0 wt%, a single-phase oil-in-water emulsion was created. Oil-in-water emulsions with an excess oil phase were observed at 10 wt%. From 20 to 70 wt%, water-in-oil emulsions (bitumen-rich) with oil-in-water emulsion (water-rich) were observed.

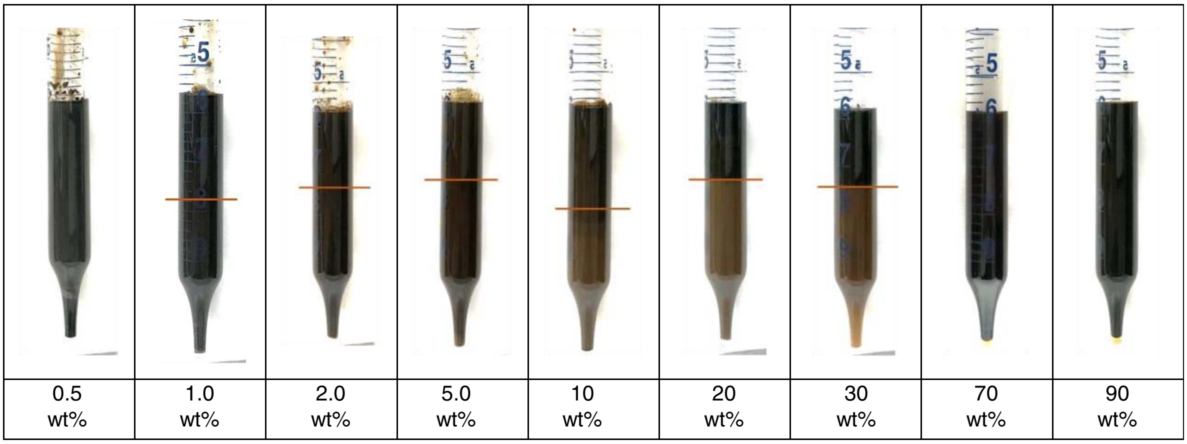

Fig. 5—Emulsion phase behavior at different DEA concentrations with 1,000 ppm salinity and WOR of 7:3, after aging at 373 K for 3 weeks. For 0.5 wt%, a single-phase oil-in-water emulsion was created. Two oil-in-water emulsions (bitumen-rich and water-rich) were observed up to 10 wt%. From 20 to 30 wt%, water-in-oil emulsions (bitumen-rich) with oil-in-water emulsion (water-rich) were observed.

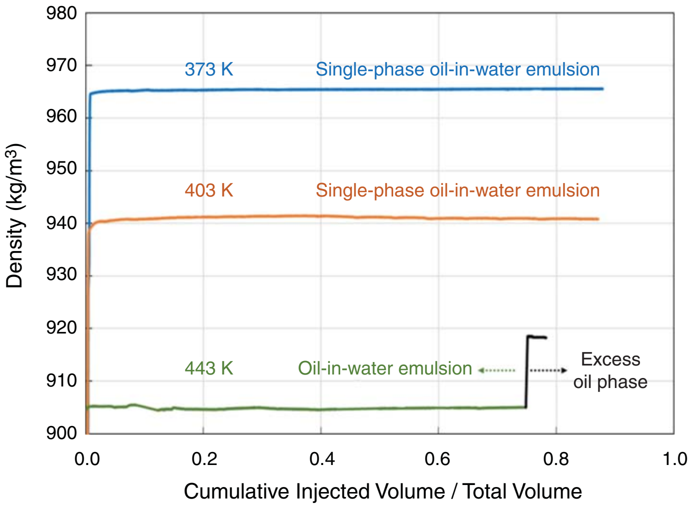

Fig. 6—Phase behavior of oil-in-water emulsions at 373, 403, and 443 K at 35 bar. Emulsion was prepared at the DEA concentration of 0.5 wt%, WOR of 7:3, and NaCl salinity of 1,000 ppm. At 373 and 403 K, a single-phase oil-in-water emulsion was detected with a constant density value. At 443 K, a phase boundary was detected with two distinct densities. The volume of the oil-in-water emulsion at 443 K was 75 vol%.

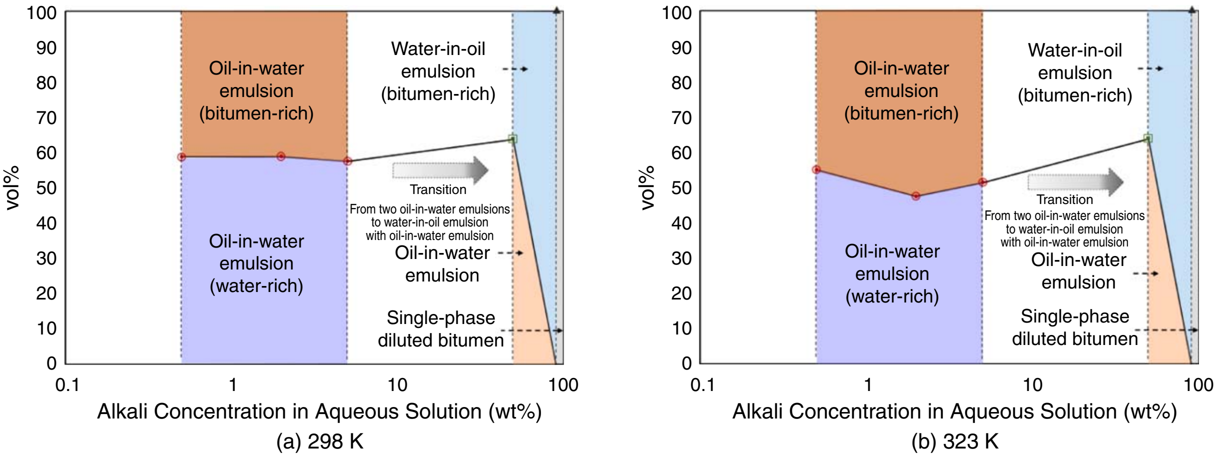

(a) 298 K

(b) 323 K

Fig. 7—Phase behavior of emulsions at 298 and 323 K. Other conditions are fixed at WOR of 7:3, 1,000 ppm, and aging for 3 weeks. Unlike the 373 K samples (Fig. 2), single-phase oil-in-water emulsions were not observed. Two oil-in-water (bitumen-rich and water-rich) emulsions were observed up to 5.0 wt% DEA concentration. At 323 K, the volume of bitumen-rich oil-in-water emulsions tends to increase compared with the sample at 298 K. For the 5.0 wt% DEA sample, the location of bitumen-rich oil-in-water emulsions was changed from the bottom to the top as temperature increased. The volume ratios of water-in-oil and oil-in-water emulsions were similar at two temperatures. ▲ = a single-phase diluted bitumen; ◉ = oil-in-water emulsions (bitumen rich) with oil-in-water emulsions (water rich); ▣ = water-in-oil emulsions (bitumen rich) with oil-in-water emulsions (water rich).

DEA concentration (wt%)		0.5	2.0	5.0	50	90
Number of phases		2	2	2	2	1
Phase	Top	Oil-in-water emulsion (water-rich)	Oil-in-water emulsion (water-rich)	Oil-in-water emulsion (water-rich)	Oil-in-water emulsion	Diluted bitumen
	Bottom	Oil-in-water emulsion (bitumen-rich)	Oil-in-water emulsion (bitumen-rich)	Oil-in-water emulsion (bitumen-rich)	Water-in-oil emulsion (bitumen-rich)	
Photo						

(a) 298 K

DEA concentration (wt%)		0.5	2.0	5.0	50	90
Number of phases		2	2	2	2	1
Phase	Top	Oil-in-water emulsion (water-rich)	Oil-in-water emulsion (water-rich)	Oil-in-water emulsion (bitumen-rich)	Oil-in-water emulsion	Diluted bitumen
	Bottom	Oil-in-water emulsion (bitumen-rich)	Oil-in-water emulsion (bitumen-rich)	Oil-in-water emulsion (water-rich)	Water-in-oil emulsion (bitumen-rich)	
Photo						

(b) 323 K

Fig. 8—Emulsion phase behavior at 1,000 ppm and WOR of 7:3 after aging for 3 weeks: (a) 298 K and (b) 323 K. These photos can be compared with those in Fig. 5, which were at 373 K after aging for 3 weeks.

298 K					
DEA Concentration (wt%)	0.5	2.0	5.0	50	90
Shear Rate (seconds^{-1})	Viscosity (cp)	Viscosity (cp)	Viscosity (cp)	Viscosity (cp)	Viscosity (cp)
0.1	76.4	–	266.8	–	86.0
0.2	134.6	–	184.5	2,001.8	79.2
0.3	144.8	–	148.4	2,088.2	49.7
0.6	105.9	447.7	130.7	2,332.6	30.3
1.0	107.0	249.7	104.7	2,217.7	21.6
1.8	82.6	163.8	82.1	1,850.7	16.1
3.2	97.4	109.6	65.3	1,610.2	13.0
5.6	84.4	97.9	58.2	1,580.6	12.5
10.0	48.3	73.6	53.4	1,531.6	14.3
17.8	37.2	59.9	50.7	1,402.2	14.5
31.6	31.0	51.3	50.0	1,355.7	14.1
56.2	31.1	43.7	48.5	1,429.3	16.1
100.0	19.5	41.9	49.2	1,375.6	21.3
323 K					
0.1	255.5	215.0	320.0	262.6	92.1
0.2	215.1	174.9	237.5	249.7	84.1
0.3	179.0	133.5	161.8	237.0	67.0
0.6	144.2	108.5	121.0	217.2	47.6
1.0	114.5	85.3	96.4	199.1	37.5
1.8	89.9	65.0	76.4	180.1	31.6
3.2	63.1	49.9	59.9	163.6	26.5
5.6	44.7	41.2	47.6	148.5	24.7
10.0	33.2	31.2	34.4	135.3	24.7
17.8	27.4	20.6	21.6	120.8	26.1
31.6	26.0	14.9	15.0	107.1	27.0
56.2	22.2	13.7	12.7	97.4	30.1
100.0	22.3	12.7	12.6	91.8	33.4

Table 3—Emulsion viscosities for samples with salinity of 1,000 ppm and WOR of 7:3 after aging for 3 weeks.

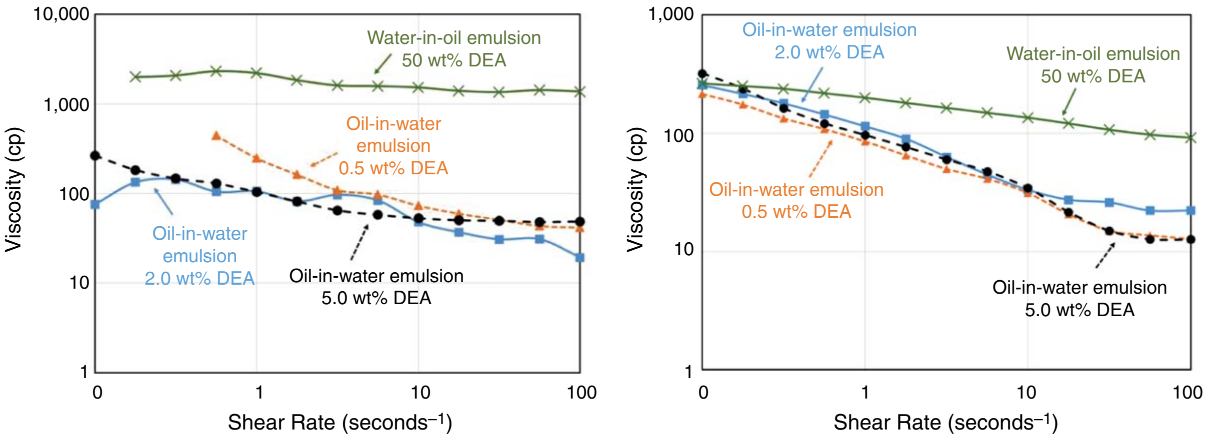

(a) 298 K

(a) 323 K

Fig. 9—Viscosity of emulsions at the DEA concentrations of 0.5, 2.0, 5.0, and 50 wt% at 298 and 323 K. For all emulsions, shear-thinning behavior was observed. Viscosity values at different shear rates are presented in Table 3.

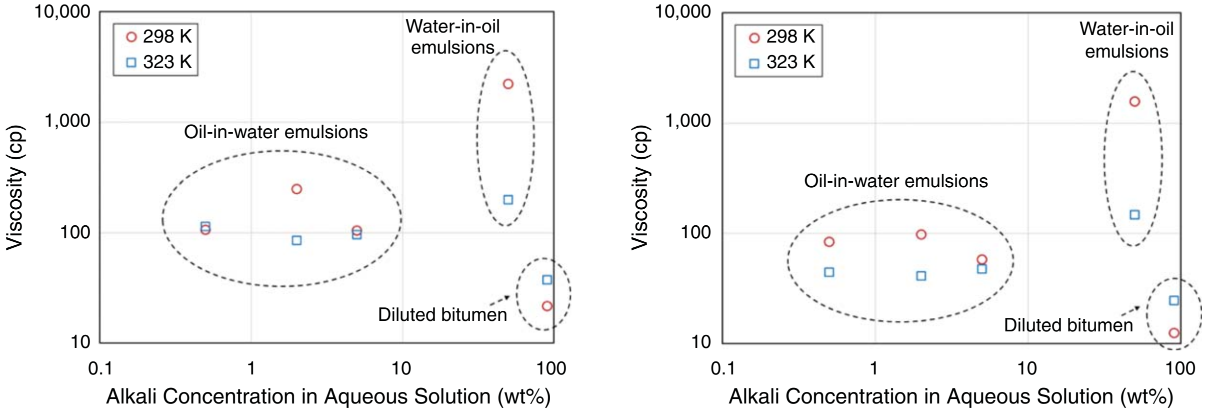

(a) Shear rate of 1.0 seconds^{-1} (b) Shear rate of 5.6 seconds^{-1}

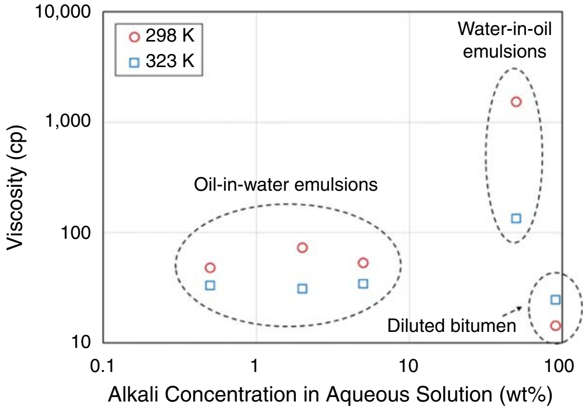

(c) Shear rate of 10.0 seconds^{-1}

Fig. 10—Viscosities of emulsions for samples with salinity of 1,000 ppm and WOR of 7:3 at three different shear rates: (a) 1.0 seconds^{-1}, (b) 5.6 seconds^{-1}, and (c) 10.0 seconds^{-1}. There are three types of fluids present: bitumen-rich oil-in-water emulsions at DEA concentrations of 0.5, 2.0, and 5.0 wt%; water-in-oil emulsions at 50 wt%; and single-phase mixture at 90 wt%.

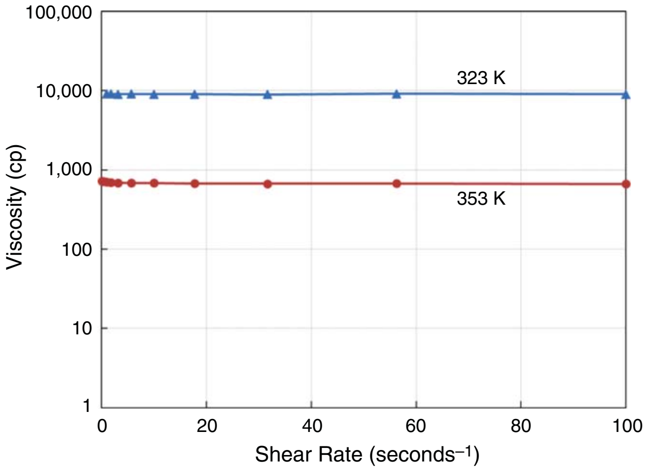

Fig. 11—Viscosity of the original bitumen at different shear rates at 323 and 353 K. Newtonian behavior was confirmed, where the bitumen viscosity was nearly independent of shear rate. The bitumen viscosity is 9,040 cp at 323 K and 690 cp at 353 K.

Conclusions

This research was concerned with the application of organic alkali as a steam additive to improve SAGD. The central question was whether adding DEA as an organic alkali can form oil-in-water emulsions that are much less viscous than the original bitumen. This research presented the fundamental data of phase behavior and viscosity for emulsions created by mixtures of Athabasca bitumen, DEA, and NaCl brine.

The phase-behavior study included 104 samples with different DEA concentrations, brine salinities, and WORs at temperatures up to 443 K. Viscosities and bitumen contents were measured for selected emulsion samples at 7:3 WOR and 1,000 ppm salinity at temperatures from 298 to 323 K. Our conclusions are the following.

1. It was possible to form oil-in-water emulsions by adding a small amount of DEA to bitumen and brine. Results showed that bitumen-rich oil-in-water emulsions tend to be dominant at low DEA concentrations and low salinities. With increasing DEA concentration, water-in-oil emulsion appeared. A single-phase solution (diluted bitumen) was observed at the DEA concentration of 90 wt% in the aqueous solution. With increasing NaCl concentration, water-in-oil-emulsion behavior tended to dominate over oil-in-water emulsion.
2. Within the conditions tested in this research, an optimal range of conditions in terms of the dominance of oil-in-water emulsion was found at low DEA concentrations for salinities less than 1,000 ppm. At a WOR of 7:3, for example, a single phase of oil-in-water emulsion was observed for 0.5, 1.0, 2.0, and 5.0 wt% DEA at zero salinity. The emulsion for 0.5 wt% DEA, 1,000 ppm NaCl, and WOR of 7:3 was observed to be a single-phase oil-in-water emulsion for temperatures up to 403 K at 35 bar. Almost all bitumen content (2.4 cm^3) in the total 8-cm^3 sample was measured from the bitumen-rich oil-in-water emulsion, the volume of which was 3.3 to 3.4 cm^3 at 0.5 to 5.0 wt% DEA at 298 K, and 3.6 to 4.2 cm^3 at 0.5 to 5.0 wt% DEA at 323 K. That is, the oil contents in these water-external emulsions were more than 70 vol% at 298 K and 57 vol% at 323 K.
3. The viscosities of these oil-in-water emulsions range between 85 and 115 cp at 1.0 seconds^{-1}, and between 31 and 34 cp at 10.0 seconds^{-1} at 323 K. At 298 K, they range between 105 and 250 cp at 1.0 seconds^{-1} and between 48 and 74 cp at 10.0 seconds^{-1}. Results show that compared with the original bitumen, bitumen-rich oil-in-water emulsions are less viscous by three to four orders of magnitude at 298 K, and less viscous by two orders of magnitude at 323 K.

Acknowledgments

We gratefully acknowledge the financial support from Japan Canada Oil Sands Limited and the Chemical Enhanced Oil Recovery Industrial Affiliates Project at the University of Texas at Austin. Author Ryosuke Okuno holds the Pioneer Corporation Faculty Fellowship in Petroleum Engineering at the University of Texas at Austin. The authors thank Gary A. Pope and Kishore K. Mohanty for sharing their laboratory equipment for this research.

References

Abdurahman, N. H., Rosli, Y. M., Azhari, N. H. et al. 2012. Pipeline Transportation of Viscous Crudes as Concentrated Oil-in-Water Emulsions. *J. Pet. Sci. Eng.* **90–91** (July): 139–144. https://doi.org/10.1016/j.petrol.2012.04.025.

Acevedo, S., Gutierrez, X., and Rivas, H. 2001. Bitumen-in-Water Emulsions Stabilized With Natural Surfactants. *J. Colloid Interf. Sci.* **242** (1): 230–238. https://doi.org/10.1006/jcis.2001.7728

Al-Sahhaf, T., Elsharkawy, A., and Fahim, M. 2008. Stability of Water-in-Crude Oil Emulsions: Effect of Oil Aromaticity, Resins to Asphaltene Ratio, and pH of Water. *Pet. Sci. Technol.* **26** (17): 2009–2022. https://doi.org/10.1080/10916460701428904

Al-Yaari, M., Hussein, I. A., Al-Sarkhi, A. et al. 2015. Effect of Water Salinity on Surfactant-Stabilized Water–Oil Emulsions Flow Characteristics. *Exp. Therm. Fluid Sci.* **64** (June): 54–61. https://doi.org/10.1016/j.expthermflusci.2015.02.001.

Ashrafizadeh, S. N. and Kamran, M. 2010. Emulsification of Heavy Crude Oil in Water for Pipeline Transportation. *J. Pet. Sci. Eng.* **71** (3–4): 205–211. https://doi.org/10.1016/j.petrol.2010.02.005.

Ashrafizadeh, S. N., Motaee, E., and Hoshyargar, V. 2012. Emulsification of Heavy Crude Oil in Water by Natural Surfactants. *J. Pet. Sci. Eng.* **86–87** (May): 137–143. https://doi.org/10.1016/j.petrol.2012.03.026.

Baek, K., Sheng, K., Argüelles-Vivas, F. J. et al. 2018. Comparative Study of Oil-Dilution Capability of Dimethyl Ether and Hexane as Steam Additives for Steam-Assisted Gravity Drainage. *SPE Res Eval & Eng*. SPE-187182-PA. (in press; posted October 2018). https://doi.org/10.2118/187182-PA.

Bahmanabadi, H., Hemmati, M., Shariatpanahi, H. et al. 2016. Phase Behavior and Rheology of Emulsions in an Alkaline/Cosolvent/Crude Oil/Brine System. *Pet. Sci. Technol.* **34** (3): 207–215. https://doi.org/10.1080/10916466.2015.1017648

Ballard, N., Salsamendi, M., Carretero, P. et al. 2015. An Investigation Into the Nature and Potential of In-Situ Surfactants for Low Energy Miniemulsification. *J. Colloid Interf. Sci.* **458** (15 November): 69–78. https://doi.org/10.1016/j.jcis.2015.07.041

Bera, A., Ojha, K., Kumar, T. et al. 2012. Phase Behavior and Physicochemical Properties of (Sodium Dodecyl Sulfate + Brine + Propan-1-ol + Heptane) Microemulsions. *J. Chem. Eng. Data* **57** (3): 1000–1006. https://doi.org/10.1021/je2013796.

Bibette, J., Roux, D., and Pouligny, B. 1992. Creaming of Emulsions: The Role of Depletion Forces Induced by Surfactant. *J. Phys. II* **2** (3): 401–424. https://doi.org/10.1051/jp2:1992141.

Bryan, J. and Kantzas, A. 2007a. Potential for Alkali-Surfactant Flooding in Heavy Oil Reservoirs Through Oil-in-Water Emulsification. Presented at the Canadian International Petroleum Conference, Calgary, 12–14 June. PETSOC-2007-134. https://doi.org/10.2118/2007-134.

Bryan, J. and Kantzas, A. 2007b. Enhanced Heavy-Oil Recovery by Alkali-Surfactant Flooding. Presented at the SPE Annual Technical Conference and Exhibition, Anaheim, California, 11–14 November. SPE-110738-MS. https://doi.org/10.2118/110738-MS.

Bryan, J., Mai, A., and Kantzas, A. 2008. Investigation Into the Processes Responsible for Heavy Oil Recovery by Alkali-Surfactant Flooding. Presented at the SPE Symposium on Improved Oil Recovery, Tulsa, 20–23 April. SPE-113993-MS. https://doi.org/10.2118/113993-MS.

Cooke, C. E. Jr., Williams, R. E., and Kolodzie, P. A. 1974. Oil Recovery by Alkaline Waterflooding. *J Pet Technol* **26** (12): 1365–1374. SPE-4739-PA. https://doi.org/10.2118/4739-PA.

Dong, M., Ma, S., and Liu, Q. 2009. Enhanced Heavy Oil Recovery Through Interfacial Instability: A Study of Chemical Flooding for Brintnell Heavy Oil. *Fuel* **88** (6): 1049–1056. https://doi.org/10.1016/j.fuel.2008.11.014.

Fan, T. and Buckley, J. S. 2007. Acid Number Measurements Revisited. *SPE J.* **12** (4): 496–500. SPE-99884-PA. https://doi.org/10.2118/99884-PA.

Fortenberry, R., Kim, D. H., Nizamidin, N. et al. 2015. Use of Cosolvents To Improve Alkaline/Polymer Flooding. *SPE J.* **2** (2): 255–266. SPE-166478-PA. https://doi.org/10.2118/166478-PA.

Gao, J., Okuno, R., and Li, H. A. 2017. An Experimental Study of Multiphase Behavior for *n*-Butane/Bitumen/Water Mixtures. *SPE J.* **22** (3): 783–798. SPE-180736-PA. https://doi.org/10.2118/180736-PA.

Ge, J., Feng, A., Zhang, G. et al. 2012. Study of the Factors Influencing Alkaline Flooding in Heavy-Oil Reservoirs. *Energy Fuels* **26** (5): 2875–2882. https://doi.org/10.1021/ef3000906.

Ghannam, M. T. and Esmail. N. 2007. Flow Enhancement of Medium-Viscosity Crude Oil. *Pet. Sci. Technol.* **24** (8): 985–999. https://doi.org/10.1081/LFT-200048166.

Ghannam, M. T., Hasan, S. W., Abu-Jdayil, B. et al. 2012. Rheological Properties of Heavy and Light Crude Oil Mixtures for Improving Flowability. *J. Pet. Sci. Eng.* **81** (January): 122–128. https://doi.org/10.1016/j.petrol.2011.12.024.

Gupta, S. C. and Zeidani, K. 2013. Surfactant-Steam Process: An Innovative Enhanced Heavy Oil Recovery Method for Thermal Applications. Presented at the SPE Heavy Oil Conference-Canada, Calgary, 11–13 June. SPE-165545-MS. https://doi.org/10.2118/165545-MS.

Hasan, S. W., Ghannam, M. T., and Esmail, N. 2010. Heavy Crude Oil Viscosity Reduction and Rheology for Pipeline Transportation. *Fuel* **89** (5): 1095–1100. https://doi.org/10.1016/j.fuel.2009.12.021.

Healy, R. N., Reed, R. L., and Stenmark, D. G. 1976. Multiphase Microemulsion Systems. *SPE J.* **16** (3): 147–160. SPE-5565-PA. https://doi.org/10.2118/5565-PA.

Jia, W. and Okuno, R. 2018. Modeling of Asphaltene and Water Associations in Petroleum Reservoir Fluids Using Cubic-Plus-Association EOS. *AIChE J.* **64** (9): 3429–3442. https://doi.org/10.1002/aic.16191.

Kar, T., Williamson, M., and Hascakir, B. 2014. The Role of Asphaltenes in Emulsion Formation for Steam Assisted Gravity Drainage (SAGD) and Expanding Solvent-SAGD (ES-SAGD). Presented at the SPE Heavy and Extra Heavy Oil Conference: Latin America, Medellín, Colombia, 24–26 September. SPE-171076-MS. https://doi.org/10.2118/171076-MS.

Kim, M., Abedin, A., Lele, P. et al. 2017. Microfluidic Pore-Scale Comparison of Alcohol- and Alkaline-Based SAGD Processes. *J. Pet. Sci. Eng.* **154** (June): 139–149. https://doi.org/10.1016/j.petrol.2017.04.025.

Kokal, S. 2005. Crude-Oil Emulsions: A State-of-the-Art Review. *SPE Prod & Fac* **20** (1): 5–13. SPE-77497-PA. https://doi.org/10.2118/77497-PA.

Kumar, R., Dao, E., and Mohanty, K. 2012. Heavy-Oil Recovery by In-Situ Emulsion Formation. *SPE J.* **17** (2): 326–334. SPE-129914-PA. https://doi.org/10.2118/129914-PA.

Liu, Q., Dong, M., Yue, X. et al. 2006. Synergy of Alkali and Surfactant in Emulsification of Heavy Oil in Brine. *Colloid. Surface. A* **273** (1–3): 219–228. https://doi.org/10.1016/j.colsurfa.2005.10.016.

Liu, Q., Dong, M., Ma, S. et al. 2007. Surfactant Enhanced Alkaline Flooding for Western Canadian Heavy Oil Recovery. *Colloid. Surface. A* **293** (1–3): 63–71. https://doi.org/10.1016/j.colsurfa.2006.07.013

Lu, C., Liu, H., Zhao, W. et al. 2017. Experimental Investigation of In-Situ Emulsion Formation To Improve Viscous-Oil Recovery in Steam-Injection Process Assisted by Viscosity Reducer. *SPE J.* **22** (1): 130–137. SPE-181759-PA. https://doi.org/10.2118/181759-PA.

Nizamidin, N., Weerasooriya, U. P., and Pope, G. A. 2015. Systematic Study of Heavy Oil Emulsion Properties Optimized With a New Chemical Formulation Approach: Particle Size Distribution. *Energy Fuels* **29** (11): 7065–7079. https://doi.org/10.1021/acs.energyfuels.5b01818.

Pal, R. 1996. Effect of Droplet Size on the Rheology of Emulsions. *AIChE J.* **42** (11): 3181–3190. https://doi.org/10.1002/aic.690421119.

Pal, R. 2000. Shear Viscosity Behavior of Emulsions of Two Immiscible Liquids. *J. Colloid Interf. Sci.* **225** (2): 359–366. https://doi.org/10.1006/jcis.2000.6776.

Pei, H., Zhang, G., Ge, J. et al. 2013. Potential of Alkaline Flooding To Enhance Heavy Oil Recovery Through Water-in-Oil Emulsification. *Fuel* **104** (February): 284–293. https://doi.org/10.1016/j.fuel.2012.08.024.

Petersen, M. A. and Grade, H. 2011. Analysis of Steam Assisted Gravity Drainage Produced Water Using Two-Dimensional Gas Chromatography With Time-of-Flight Mass Spectrometry. *Ind. Eng. Chem. Res.* **50** (21): 12217–12224. https://doi.org/10.1021/ie200531h.

Razi, M., Sinha, S., Waghmare, P. R. et al. 2016. Effect of Steam-Assisted Gravity Drainage Produced Water Properties on Oil/Water Transient Interfacial Tension. *Energy Fuels* **30** (12): 10714–10720. https://doi.org/10.1021/acs.energyfuels.6b01686.

Robins, M. M. and Hibberd, D. J. 1998. Emulsion Flocculation and Creaming. In *Modern Aspects of Emulsion Science*, ed. B. P. Binks, Chap. 4, 115–144. London: Royal Society of Chemistry.

Salager, J. L., Loaiza-Maldonado, I., Minana-Perez, M. et al. 1982. Surfactant-Oil-Water Systems Near the Affinity Inversion Part I: Relationship Between Equilibrium Phase Behavior and Emulsion Type and Stability. *J. Dispers. Sci. Technol.* **3** (3): 279–292. https://doi.org/10.1080/01932698208943642

Schorling, P.-C., Kessel, D. G., and Rahimian, I. 1999. Influence of the Crude Oil Resin/Asphaltene Ratio on the Stability of Oil/Water Emulsions. *Colloid. Surface. A* **152** (1–2): 95–102. https://doi.org/10.1016/S0927-7757(98)00686-4.

Sharma, J. and Gates, I. D. 2010. Multiphase Flow at the Edge of a Steam Chamber. *Can. J. Chem. Eng.* **88** (3): 312–321. https://doi.org/10.1002/cjce.20280.

Sharma, J., Panthi, K., and Mohanty, K. K. 2018. Surfactant-Less Alkali-Cosolvent-Polymer Floods for an Acidic Crude Oil. *Fuel* **215** (1 March): 484–491. https://doi.org/10.1016/j.fuel.2017.11.079.

Sheng, J. J. 2015. Investigation of Alkaline–Crude Oil Reaction. *Petroleum* **1** (1): 31–39. https://doi.org/10.1016/j.petlm.2015.04.004.

Sheng, K., Argüelles-Vivas, F. J., Baek, K. H. et al. 2018. An Experimental Study of Emulsion Flow in Alkaline Solvent Coinjection With Steam for Heavy-Oil/Bitumen Recovery. Presented at the SPE Improved Oil Recovery Conference, Tulsa, 14–18 April. SPE-190224-MS. https://doi.org/10.2118/190224-MS.

Shi, X. and Okuno, R. 2018. Analytical Solution for Steam-Assisted Gravity Drainage With Consideration of Temperature Variation Along the Edge of a Steam Chamber. *Fuel* **217** (1 April): 262–274. https://doi.org/10.1016/j.fuel.2017.12.110.

Srivastava, P. and Castro, L. 2011. Successful Field Application of Surfactant Additives To Enhance Thermal Recovery of Heavy Oil. Presented at the SPE Middle East Oil and Gas Show and Conference, Manama, Bahrain, 25–28 September. SPE-140180-MS. https://doi.org/10.2118/140180-MS.

Tagavifar, M., Herath, S., Weerasooriya, U. et al. 2017. Measurement of Microemulsion Viscosity and Its Implications for Chemical Enhanced Oil Recovery. *SPE J.* **23** (1): 66–83. SPE-179672-PA. https://doi.org/10.2118/179672-PA.

Venkatramani, A. V. and Okuno, R. 2018. Mechanistic Simulation Study of Expanding-Solvent Steam-Assisted Gravity Drainage Under Reservoir Heterogeneity. *J. Pet. Sci. Eng.* **169** (October): 146–156. https://doi.org/10.1016/j.petrol.2018.04.074.

Winsor, P. A. 1948. Hydrotropy, Solubilisation and Related Emulsification Processes. *Trans. Faraday Soc.* **44:** 376–398. https://doi.org/10.1039/TF9484400376.

Xia, L., Lu, S., and Cao, G. 2004. Stability and Demulsification of Emulsions Stabilized by Asphaltenes or Resins. *J. Colloid Interf. Sci.* **271** (2): 504–506. https://doi.org/10.1016/j.jcis.2003.11.027.

Xiao, R., Teletzke, G. F., Lin, M. W. et al. 2017. A Novel Mechanism of Alkaline Flooding To Improve Sweep Efficiency for Viscous Oils. Presented at the SPE Annual Technical Conference and Exhibition, San Antonio, Texas, 9–11 October. SPE-187366-MS. https://doi.org/10.2118/187366-MS.

Yan, Z., Elliott, J. A. W., and Masliyah, J. H. 1999. Roles of Various Bitumen Components in the Stability of Water-in-Diluted-Bitumen Emulsions. *J. Colloid Interf. Sci.* **220** (2): 329–337. https://doi.org/10.1006/jcis.1999.6533.

Yang, X., Verruto, V. J., and Kilpatrick, P. K. 2007. Dynamic Asphaltene-Resin Exchange at the Oil/Water Interface: Time-Dependent W/O Emulsion Stability for Asphaltene/Resin Model Oils. *Energy Fuels* **21** (3): 1343–1349. https://doi.org/10.1021/ef060465w.

Yarranton, H. W., Hussein, H., and Masliyah, J. H. 2000. Water-in-Hydrocarbon Emulsions Stabilized by Asphaltenes at Low Concentrations. *J. Colloid Interf. Sci.* **228** (1): 52–63. https://doi.org/10.1006/jcis.2000.6938.

Zhang, J., Tian, D., Lin, M. et al. 2016. Effect of Resins, Waxes and Asphaltenes on Water-Oil Interfacial Properties and Emulsion Stability. *Colloid. Surface. A* **507** (20 October): 1–6. https://doi.org/10.1016/j.colsurfa.2016.07.081.

Zhu, D. and Okuno, R. 2016. Multiphase Isenthalpic Flash Integrated With Stability Analysis. *Fluid Phase Equilibr.* **423** (15 September): 203–219. https://doi.org/10.1016/j.fluid.2016.04.005.

Kwang Hoon Baek is a PhD degree candidate in petroleum engineering in the Hildebrand Department of Petroleum and Geosystems Engineering at the University of Texas at Austin. His research interests include thermal enhanced oil recovery (EOR), chemical EOR, multiphase behavior, and properties of petroleum fluids. Baek holds a bachelor's degree in chemical engineering from Yonsei University, South Korea, and a master's degree in science and technology policy from Korea Advanced Institute of Science and Technology. He is a member of SPE.

Francisco Javier Argüelles-Vivas is a post-doctoral-degree fellow in the Hildebrand Department of Petroleum and Geosystems Engineering at the University of Texas at Austin. Previously, he worked as a reservoir engineer at the Mexican Petroleum Institute for 2 years. Argüelles-Vivas' current research interests are EOR methods for conventional/unconventional reservoirs, formation damage, phase behavior of bitumen/heavy-oil/solvent mixtures, pore-scale modeling, and carbon dioxide sequestration. He holds a bachelor's degree in chemical engineering from the Metropolitan Autonomous University, Mexico; a master's degree in petroleum engineering from the Mexican Petroleum Institute; and a PhD degree in petroleum engineering from the University of Alberta. Argüelles-Vivas is a member of SPE and currently serves as a technical reviewer for *SPE Journal*.

Ryosuke Okuno is an associate professor in the Hildebrand Department of Petroleum and Geosystems Engineering at the University of Texas at Austin. He has 7 years of industrial experience as a reservoir engineer, and is a registered professional engineer in Alberta, Canada. Okuno's research and teaching interests include EOR, thermal oil recovery, unconventional oil and gas resources, numerical reservoir simulation, thermodynamics, multiphase behavior, and applied mathematics. He is a recipient of the 2012 SPE Petroleum Engineering Junior Faculty Research Initiation Award, is an associate editor for *SPE Journal*, and holds the Pioneer Corporation Faculty Fellowship in Petroleum Engineering at the University of Texas at Austin. Okuno holds bachelor's and master's degrees in geosystem engineering from the University of Tokyo, and a PhD degree in petroleum engineering from the University of Texas at Austin.

Kai Sheng is a PhD degree candidate in petroleum engineering in the Hildebrand Department of Petroleum and Geosystems Engineering at the University of Texas at Austin. His research interests include thermal EOR, numerical reservoir simulation, and multiphase behavior and fluid properties of heavy oil and bitumen. Sheng holds a bachelor's degree from the China University of Petroleum, East China, and a master's degree from the University of Alberta, both in petroleum engineering. He is a member of SPE.

Himanshu Sharma is a post-doctoral-degree fellow in the Hildebrand Department of Petroleum and Geosystems Engineering at the University of Texas at Austin. His research interests include interfacial phenomena and reactive transport in porous media, particularly during alkali/surfactant/polymer flooding and wettability alteration. Sharma holds a PhD degree in petroleum engineering from University of Texas at Austin, and bachelor's and master's degrees in chemical engineering from the Indian Institute of Technology.

Upali P. Weerasooriya is a senior research scientist and director of surfactant development at the Center for Petroleum and Geosystems Engineering at the University of Texas at Austin, and is a founder of Ultimate EOR Services. Since 2011, he has also been president and chief executive officer of the Dr. Upali Weerasooriya Foundation, an approved charitable organization. Previously, Weerasooriya served as the vice president of technology and the chief technical officer at Harcros Chemical Company. He is the holder of more than 60 US patents on surfactant technology. Weerasooriya holds a PhD degree in chemistry from the University of Texas at Austin. He is a member of SPE.